Science Advances

AAAS

advances.sciencemag.org/cgi/content/full/4/2/eaao0926/DC1

Supplementary Materials for

Growing old, yet staying young: The role of telomeres in bats' exceptional longevity

Nicole M. Foley, Graham M. Hughes, Zixia Huang, Michael Clarke, David Jebb, Conor V. Whelan, Eric J. Petit, Frédéric Touzalin, Olivier Farcy, Gareth Jones, Roger D. Ransome, Joanna Kacprzyk, Mary J. O'Connell, Gerald Kerth, Hugo Rebelo, Luísa Rodrigues, Sébastien J. Puechmaille, Emma C. Teeling

Published 7 February 2018, *Sci. Adv.* **4**, eaao0926 (2018)
DOI: 10.1126/sciadv.aao0926

This PDF file includes:

- fig. S1. LMMs fitted to each data set after the removal of the 0-age cohort.
- fig. S2. Analysis of *P* values arising from 100 jackknifed models of telomere length versus age.
- fig. S3. Analysis of slope values arising from 100 jackknifed models of telomere length versus age.
- fig. S4. Randomly subsampled *M. myotis* and *R. ferrumequinum* data sets containing equal numbers of samples per age cohort recapitulate results from Fig. 2 and show that telomeres shorten in *R. ferrumequinum*, but we do not detect a significant relationship between rTL and age in *M. myotis*.
- fig. S5. Upper quartile regression analysis.
- fig. S6. Tree topology used for selective pressure analyses.
- fig. S7. Schematic depicting steps in the OH-SNAP workflow to automate CodeML analysis.
- fig. S8. STRING protein-protein interaction network for 14 significantly DEGs in *Myotis* bats compared to all other mammals.
- References (*71–94*)

Supplementary Text

Telomere Length Analysis

The jackknife analyses confirmed the robustness of our results. The analysis returned a significant relationship between rTL and age in 90% of replicates for *R. ferrumequinum* and 100% in *Miniopterus schreibersii* (fig. S1a-b). In the case of *M. myotis* and *M. bechsteinii* a significant result was returned in only 5% and 2% of replicates respectively (fig. S1c-d). Direct jackknife comparison of the two largest data sets, *M. myotis* and *R. ferrumequinum* containing equal age cohorts and equal numbers of samples per age cohort (1-6+ yrs; n=91) recapitulated initial results: show that telomeres shorten in *R. ferrumequinum* but do not detect a significant relationship between rTL and age in *M. myotis* (fig. S3).

The LMMs fitted to each data set with the 0 age cohort removed recapitulate the results from data sets analysed with the 0 age cohort included (fig. S7). Detailed model outputs are described in table S8. These results suggest that the difference in significance between models fitted to *Myotis* bats and all other bats is not simply due to differences in effect size. The conditional r^2 values suggest that most of the variance in the *R. ferrumequinum* data set is captured by the model ($r^2_c = 0.919$), while less variance is explained by models fitted to either *Myotis* data set (*M. bechsteinii* $r^2_c = 0.85$; *M.myotis* $r^2_c = 0.422$). This suggests that potentially some unknown factor, besides age, influences telomere dynamics in these species.

Tests of Selective Pressure Variation

Our analyses of selective pressure variation did not detect evidence of positive or divergent selection on the branches leading to *R. ferrumequinum* (Fig. 4d and table S7). Genome quality is a factor potentially impacting our results in *R. ferrumequinum*. This unannotated genome is low coverage (17X) and mining with our custom MAKER pipeline resulted in far fewer targeted sequences recovered (113/225) (Fig. 4). *SETX* and *CCT5*, which were shown to be evolving under divergent selection in the genus *Myotis* and *Miniopterus natalensis* respectively, are included in our *R. ferrumequinum* data set (*MYC*, *ATM* and *HNRNPU* could not be successfully mined) but are not significant, suggesting that other longevity mechanisms may have evolved in this species. Improvements to the existing *R. ferrumequinum* genome will aid our understanding of mechanisms contributing to longevity in this species. A *Rhinolophus sinicus* genome was published after completion of this analysis (*71*), inclusion of this data in future analyses is recommended. While *TEP1* and *TERF1* have been shown to be evolving under positive selection in the naked mole rat (*72*), we do not find the same result in our analyses.

Given recent critical assessments of genome scan studies (*73*), to account for differences in genome coverage and quality across our eutherian data set, only genes which were significantly recovered through analysis of the RefSeq and RefSeq + MAKER data sets, after FDR were considered robust for all selection tests. This somewhat conservative approach ensured our results were robust to the removal and addition of data.

Our selective pressure analyses on the *Miniopterus natalensis* branch showed that *CCT5, HNRNPU* and *LIG1*evolved under divergent selection in *Miniopterus natalensis* (Fig. 4b and table S7). *LIG1* is a DNA ligase that is a key component of replication, recombination and repair of DNA, which seals double stranded breaks (*74*). In addition to its role in telomere maintenance *CCT5* is a subunit of the chaperonin TRiC which maintains proteostasis through facilitating protein folding and sequestering unfolded proteins (*75*). Similarly *HNRNPU,* from the hnRNP gene family, is involved in a variety of

proteostatic processes that influence gene expression through the metabolism, regulation and trafficking of RNA (*76*). These particular results are supported by previous studies which have shown a role for improved proteostasis in longer lived species, compared to short-lived related species (*77*). Telomere shortening with age in the closely related *Miniopterus schreibersii* coupled with divergent evolution observed in these telomere maintenance genes, suggest that potentially enhanced proteostasis has played a greater role in the evolution of longevity in the genus *Miniopterus* than telomere maintenance, compared to *Myotis* species. Although, as this study targets only a subset of genes involved in telomere maintenance, it would be informative to perform a genome-wide selective pressure analysis as well as transcriptomic analyses in *Miniopterus* species to fully elucidate if enhanced proteostasis played a role in the evolution of *Miniopterus* species.

Previous studies have proposed a link between immunity, longevity and flight in bats (*78*), a similar trend is observed in our results. *MYC*, which is evolving under divergent selection in the ancestral bat branch, has been shown to play a key role in the development, differentiation and activation of immune cells. Previous studies of microRNAs have posited a link between inflammation, replicative senescence and longevity (*22, 79*). In the genus *Myotis*, human experiments have shown that *ATM* regulates *NF-κB* which is key in triggering the adaptive and innate immune responses (*80*), while *SETX* has been shown to attenuate the magnitude of the host response to viral infection and controls viral biogenesis (*81*). In *Miniopterus natalensis HNRNPU* enhances the expression of the pro-inflammatory cytokine *TNFα* (*82*). Previous analyses which detected positive selection in *ATM* along the ancestral bat branch contained two species, *Pteropus alecto* and *Myotis davidii (78).* Results presented here, suggest that this result may be driven by the presence of *M. davidii* in their data set, as here we show *ATM* is evolving under divergent selection in the genus *Myotis*, but not along the bat ancestral branch. Our results provide further targets with which to test support for hypotheses relating immunity, longevity and flight in bats (*78*).

Comparative Transcriptomic Analysis of Telomere Maintenance Genes

The expression levels of telomere maintenance genes were investigated and compared between *Myotis* bats and seven other mammalian species across four tissue types: blood, kidney, liver and brain. Pairwise comparisons indicated that a wide range of telomere maintenance genes (36.5% ~ 70.9%) were differentially expressed (FDR < 0.05) between bat and other mammal species. A significant number of DEGs were downregulated in bats compared to cow and whale, while DEGs were much more up-regulated in bats compared to human, mouse, rat, naked mole rat and pig (table S9). The STRING protein-protein interaction network showed interactions between 14 upregulated genes (fig. S8) and indicated an isolated interaction between GNL3L and SSB (not shown). The resulting network showed functional enrichment for 54 Biological Process GO terms and 6 KEGG pathways (tables S10-11). Besides GO terms associated with telomere maintenance, after FDR correction the network analysis showed significant functional enrichment (p-value < 0.05) for several biological processes involved in DNA repair (tables S10-11).

table S1. Details of capture and sampling permits for each population included in this study.

Species	Country	Permit(s)	Permit Issued By	Permit Holder	Duration	Access to field sites facilitated by:
Myotis myotis	France	Arrêté préfectoral (18/07/2013 & 05/08/2013)	Préfet du Morbihan	Eric Petit, Frédéric Touzalin and Sébastien Puechmaille	15th June - 15th September; 2013-2017 inclusive	local authorities in collaboration with Bretagne Vivante
		Arrêté préfectoral (26/09/2016)	Préfet du Morbihan	Frédéric Touzalin and Sébastien Puechmaille	26th August 2016 - 31st December 2020	local authorities in collaboration with Bretagne Vivante
Rhinolophus ferrumequinum	UK	2015-11974-SCI-SCI PPL30/30 25	Natural England/Home Office	Roger Ransome / Gareth Jones	2014-2016	Woodchester Mansion Trust
Myotis bechsteinii	Germany	55.1-8642.01-2/00 55.2-2531.01-47/11 55.2-2532-2-20	Government of Lower Frankonia	Gerald Kerth	2011-2020	Local forest department
Miniopterus schreibersii	Portugal	452/2016/CAPT	Institute for Nature Conservation and Forestry	Hugo Rebelo	2016	N/A

table S2. Detailed model input and output. A suite of models were fitted to each data set: a linear model (LM), a parabolic model (PM), a piecewise-linear model (PLM) and a linear mixed model (LMM). The best scoring AIC value is shown in bold. All models were analysed using rTL as the response variable and Age as the explanatory variable. Detailed output for the best model is shown.

Species	Models Tested	Ranked AIC	Best Model	Random Variables	Fixed Effect	Estimate	Standard Error	t-value	*p*-value
Myotis	LMM	**79.17**	LMM	DNA Plate, Assay Plate	Intercept	1.492	0.092	16.173	0
myotis	PM	142.56		and Year Sampled	Age	-0.019	0.013	-1.409	0.161
	PLM	143.61							
	LM	145.16							
Myotis	LMM	**107.93**	LMM	DNA Plate, Assay Plate	Intercept	2.817	0.649	4.342	0.213
bechsteinii	LM	158.78		and Year Sampled	Age	-0.021	0.019	-1.119	0.27
	PM	160.41							
	PLM	162.73							
Rhinolophus	LMM	**-350.24**	LMM	DNA Plate and Assay Plate	Intercept	0.986	0.174	5.671	0.105
ferrumequinum	PLM	-133.38			Age	-0.004	0.001	-3.268	0.001***
	PM	-105.07							
	LM	-85.56							
Miniopterus	LM	**-41.24**	LM	NA	Intercept	1.738	0.034	51.559	0
schreibersii	PM	-40.43			Age	-0.024	0.005	-5.041	0.000***
	PLM	-38.42							
	LMM	-23.69							

table S3. List of taxa and tissues used in the comparative transcriptome analysis of telomere maintenance genes. * followed by a tissue indicates that there is no publication associated with this data set.

	Common Name	**Blood**	**Kidney**	**Liver**	**Brain**	**Data Source**
Myotis brandtii	Brandt's bat	NA	2	2	1	(*83*)
Myotis myotis	Greater mouse-eared bat	4	NA	NA	NA	(*49*)
Bos taurus	Cow	NA	4	4	4	(*84*)
Sus scrofa	Pig	3	1	2	NA	(*85-87*)
Balaena mysticetus	Bowhead whale	NA	4	3	NA	(*88*)
Homo sapiens	Human	6	3	4	3	(*89*, *90*) *liver; *brain;
Mus musculus	Mouse	4	2	3	3	(*91*, *92*); The ENCODE Consortium 2011 (kidney and liver data)
Rattus norvegicus	Rat	NA	3	3	3	(*93*)
Heterocephalus glaber	Naked mole rat	NA	2	3	3	(*72*, *94*); *kidney;

table S4. Summary of alignment details for the RefSeq and RefSeq + MAKER data sets used in the selective pressure variation tests of telomere maintenance genes.

	Ref Seq + MAKER Data		RefSeq	
Gene	**No. of Taxa**	**Alignment Length**	**No. of Taxa**	**Alignment Length**
ABL1	45	3276	45	3276
ABL2	47	3375	46	3375
ACD	45	1290	45	1290
AKT1	38	1431	37	1431
APEX1	52	951	51	951
ATM	45	9138	44	9138
ATP5C1	50	825	50	825
ATR	43	7917	43	7884
ATRX	44	7314	43	7314
AURKB	49	1020	49	1020
BCL2	47	582	44	582
BLM	49	4242	48	4233
BRCA1	49	2196	45	2193
BRCA2	44	9963	43	9951
BRIP1	43	3471	43	3459
CBX1	49	543	48	543
CBX3	46	546	44	546
CBX5	49	573	49	573
CCDC79	45	2133	45	2127
CCDC155	49	1350	48	1350
CCT2	52	1578	52	1578
CCT3	51	1629	50	1629
CCT4	50	1581	50	1581
CCT5	50	1602	49	1599
CCT6A	50	1581	49	1581
CCT7	52	1620	52	1614
CCT8	50	1548	50	1545
CD19	47	1506	43	1497
CDC45	50	1668	50	1668
CDK2	52	873	51	873
CDKN1A	51	474	51	474
CHEK1	52	1251	52	1248
CHEK2	46	1506	46	1503
CTC1	49	3558	48	3546
CTNNB1	52	2337	52	2337
DCLRE1A	51	3075	51	3075
DCLRE1B	49	1551	48	1551
DCLRE1C	44	1743	41	1740
DHX36	49	2865	49	2865
DMC1	49	1017	49	1017

	Ref Seq + MAKER Data		RefSeq	
Gene	**No. of Taxa**	**Alignment Length**	**No. of Taxa**	**Alignment Length**
DNA2	44	3084	43	3084
DOT1L	46	4137	43	4134
DPY30	48	291	46	291
DYDC1	47	507	47	501
DYDC2	41	366	40	366
EGF	44	3285	42	3255
EID3	50	933	50	933
EME1	51	1698	51	1686
ERCC1	49	849	48	846
EXO1	46	2433	46	2433
FANCA	45	3690	42	3669
FANCC	45	1608	44	1608
FANCE	47	1218	46	1218
FANCI	48	3915	48	3909
FANCL	44	1095	44	1092
FBXO4	47	972	47	972
FEN1	51	1137	51	1137
GAR1	45	507	44	504
GNL3	51	1566	51	1563
GNL3L	46	1650	45	1650
H2AFX	44	360	44	360
H2AFY	45	1107	44	1107
H3F3A	45	408	43	408
H3F3B	45	408	44	408
HAT1	49	1257	49	1257
HDAC8	45	993	44	993
HMBOX1	42	1260	42	1260
HMGA2	35	246	34	246
HNRNPA1	48	1113	45	1113
HNRNPA2B1	48	1056	48	1056
HNRNPC	50	879	50	879
HNRNPD	45	771	45	771
HNRNPU	47	1776	47	1776
HORMAD1	49	1170	49	1170
HSP90AA1	46	2184	46	2184
HSPA1L	34	1917	33	1917
IGF1	47	396	46	339
KRAS	50	450	50	450
LIG1	43	2634	43	2634
MAEL	47	1290	47	1287
MAJIN	33	291	33	288
MAP2K7	49	1122	47	1122
MAP3K4	43	4326	40	4320

	Ref Seq + MAKER Data		RefSeq	
Gene	**No. of Taxa**	**Alignment Length**	**No. of Taxa**	**Alignment Length**
MAPK1	43	789	42	789
MAPK3	45	795	45	795
MAPK15	39	951	38	948
MAPKAPK5	50	1362	50	1362
MEI1	46	3588	45	3588
MEI4	41	1140	41	1131
MEIOB	44	1281	44	1281
MLH1	50	2241	50	2235
MLH3	50	4281	50	4275
MME	49	2235	48	2235
MRE11A	46	2010	45	2004
MSH2	48	2781	48	2778
MSH3	44	3165	42	3156
MSH4	45	2601	44	2487
MUS81	52	1581	52	1581
MUTYH	48	1518	48	1518
MYC	45	1305	45	1302
NABP2	50	612	49	612
NAT10	49	3069	49	3069
NBN	48	1875	45	1803
NCL	46	1818	44	1815
NDC1	46	2010	43	2010
NEK2	48	1311	47	1227
NEK7	44	888	44	888
NHP2	50	456	50	453
NOP10	46	174	45	174
NSMCE1	51	759	51	759
NSMCE2	43	723	41	720
NSMCE4A	44	837	43	834
NUP98	50	5361	50	5361
OBFC1	49	1059	48	1059
PALB2	47	1446	46	1443
PARP1	48	2874	48	2874
PARP2	51	1623	51	1608
PARP3	46	1575	46	1575
PARP4	40	4032	39	4011
PAX8	43	771	43	771
PCNA	49	783	49	783
PIF1	45	1407	45	1407
PINX1	42	909	41	909
PKIB	46	207	45	207
PLA2R1	47	4257	46	4257
PLK1	47	1704	47	1704

	Ref Seq + MAKER Data		RefSeq	
Gene	**No. of Taxa**	**Alignment Length**	**No. of Taxa**	**Alignment Length**
PML	43	2397	42	2394
PMS1	47	2775	47	2775
PMS2	42	2430	41	2373
PNKP	47	1143	47	1143
POLA1	44	4347	42	4344
POLA2	49	1755	49	1755
POLD1	47	2823	47	2820
POLD2	50	1392	50	1392
POLD3	48	1365	47	1365
POLD4	47	276	47	276
POLE2	41	1533	41	1533
POLE	46	6618	45	6618
POT1	45	1902	45	1845
PPARG	46	1422	46	1422
PPP2R1A	42	1764	42	1764
PPP2R1B	47	1485	47	1485
PRIM1	48	1239	48	1239
PRIM2	45	1233	45	1224
PRKCA	44	1806	43	1806
PRKCB	39	1581	39	1581
PRKCQ	48	2091	48	2091
PRKDC	42	12327	41	12327
PTGES3	50	477	49	477
PURA	39	654	38	654
RAD17	47	2013	46	2010
RAD21L1	46	1659	46	1656
RAD50	46	3924	46	3924
RAD51	50	1017	49	1017
RAD51C	45	1059	42	1056
RAD51D	48	858	48	858
RAPGEF1	46	3195	45	3195
RASSF1	45	660	45	660
RB1	45	2433	44	2430
RBL2	51	3174	51	3174
REC8	49	1575	49	1575
RFC1	46	3411	46	3408
RFC2	47	936	47	936
RFC3	48	1056	48	1056
RFC4	51	1089	51	1089
RFC5	51	996	51	996
RIF1	48	7260	48	7245
RNF8	49	1326	49	1326
RPA1	49	1791	49	1791

	Ref Seq + MAKER Data		RefSeq	
Gene	**No. of Taxa**	**Alignment Length**	**No. of Taxa**	**Alignment Length**
RPA2	48	795	48	795
RPA3	48	348	47	348
RTEL1	46	3132	45	3111
SAMHD1	44	1755	44	1722
SDE2	52	1326	52	1320
SETX	48	7845	46	7758
SIRT2	51	1053	51	1047
SIRT6	45	852	45	849
SLX1A	42	723	42	723
SLX4	48	4647	48	4560
SMC5	45	3270	44	3270
SMC6	50	3279	50	3273
SMG1	46	10881	46	10881
SMG5	47	3036	47	3036
SMG6	47	4149	46	4149
SP1	48	2289	45	2289
SPATA22	40	1083	39	1083
SPO11	49	1167	49	1167
SRC	47	1575	47	1575
SSB	49	1209	45	1209
STAG3	48	3591	47	3588
SUN1	46	2112	46	2076
SUV39H1	44	1215	44	1215
SUV39H2	51	1050	49	1050
SYCP1	45	2916	44	2916
TCP1	49	1665	48	1665
TDG	45	1119	45	1116
TELO2	49	2286	47	2283
TEN1	45	309	44	303
TEP1	47	7434	47	7434
TERB2	42	654	42	654
TERF1	43	1245	43	1062
TERF2	43	1377	43	1377
TERF2IP	47	1140	44	1128
TERT	42	2313	41	2310
TEX15	51	8286	50	8283
TFIP11	50	2502	50	2502
TGFB1	46	1005	46	999
TINF2	41	1209	41	1209
TNKS1BP1	46	4692	44	4626
TNKS2	48	2913	48	2913
TNKS	45	3780	45	3780
TP53	47	1080	47	1065

	Ref Seq + MAKER Data		RefSeq	
Gene	**No. of Taxa**	**Alignment Length**	**No. of Taxa**	**Alignment Length**
TP53BP1	43	5898	43	5898
TPP1	48	1659	47	1659
TREX1	44	933	44	933
UBE2B	51	450	50	450
UPF1	41	3105	40	3105
USP7	50	3150	50	3150
WNT16	50	972	50	963
WRAP53	49	1542	48	1539
WRN	45	4119	43	4104
XRCC3	39	891	38	888
XRCC5	45	2097	45	2097
XRCC6	51	1806	51	1803
YLPM1	39	6330	39	6330

table S5. List of eutherian mammal genomes mined for the selective pressure heterogeneity analyses.

Species	Common Name	Order	Max. Lifespan (yrs)	Genome mined via MAKER pipeline	Genome Version
Dasypus novemcinctus	Armadillo	Cingulata	22.3	FALSE	3
Choloepus hoffmanni	Sloth	Pilosa	NA	TRUE	2.0.1
Trichechus manatus latirostris	Manatee	Sirenia	65	FALSE	1
Loxodonta africana	African Elephant	Proboscidea	65	FALSE	3
Procavia capensis	Hyrax	Hyracoidea	14.8	TRUE	2
Orycteropus afer	Aardvark	Tubulidentata	29.8	FALSE	1
Elephantulus edwardii	Elephant shrew	Macroscelidea	NA	FALSE	1
Echinops telfairi	Tenrec	Afrosoricida	19	FALSE	2
Condylura cristata	Star-nosed mole	Eulipotyphla	2.5	FALSE	1
Erinaceus europaeus	European mole	Eulipotyphla	11.7	FALSE	2
Sorex araneus	Shrew	Eulipotyphla	3.2	FALSE	2

Species	Common Name	Order	Max. Lifespan (yrs)	Genome mined via MAKER pipeline	Genome Version
Eidolon helvum	Straw-coloured fruit bat	Chiroptera	21.8	TRUE	1
Pteropus alecto	Black flying fox	Chiroptera	19.7	FALSE	1
Pteropus vampyrus	Large flying fox	Chiroptera	20.9	FALSE	2
Rhinolophus ferrumequinum	Greater horseshoe bat	Chiroptera	30.5	TRUE	1
Megaderma lyra	Greater false vampire bat	Chiroptera	14	TRUE	1
Pteronotus parnellii	Parnell's moustached bat	Chiroptera	NA	TRUE	1
Miniopterus natalensis	Natal long-fingered bat	Chiroptera	NA	FALSE	1
Eptesicus fuscus	Big brown bat	Chiroptera	19	FALSE	1
Myotis brandtii	Brandt's bat	Chiroptera	41	FALSE	1
Myotis myotis	Greater mouse-eared bat	Chiroptera	37.1	TRUE	1
Myotis davidii	David's myotis	Chiroptera	NA	FALSE	1
Myotis lucifugus	Little brown bat	Chiroptera	34	FALSE	2

Species	Common Name	Order	Max. Lifespan (yrs)	Genome mined via MAKER pipeline	Genome Version
Balaenoptera acutorostrata	Minke whale	Cetartiodactyla	50	FALSE	1
Bison bison	Bison	Cetartiodactyla	33.5	FALSE	1
Camelus dromedarius	Camel	Cetartiodactyla	28.4	FALSE	1
Lipotes vexillifer	River Dolphin	Cetartiodactyla	24	FALSE	1
Orcinus orca	Orca whale	Cetartiodactyla	90	FALSE	1.1
Ovis aries	Sheep	Cetartiodactyla	22.8	FALSE	4
Sus scrofa	Pig	Cetartiodactyla	27	FALSE	10.2
Vicugna pacos	Llama	Cetartiodactyla	25.8	FALSE	2.0.2
Ailuropoda melanoleuca	Panda	Carnivora	36.8	FALSE	1
Canis lupus familiaris	Dog	Carnivora	20.6	FALSE	3.1
Felis catus	Cat	Carnivora	30	FALSE	8
Mustela putorius	Ferret	Carnivora	11.1	FALSE	1

Species	Common Name	Order	Max. Lifespan (yrs)	Genome mined via MAKER pipeline	Genome Version
Manis pentadactyla	Pangolin	Pholidota	NA	TRUE	1.1.1
Ceratotherium simum	Rhinoceros	Perissodactyla	45	FALSE	1
Equus caballus	Horse	Perissodactyla	57	FALSE	2
Tupaia chinensis	Tree shrew	Scandentia	NA	FALSE	1
Heterocephalus glaber	Naked mole rat	Rodentia	31	FALSE	1
Jaculus jaculus	Lesser Egyptian jerboa	Rodentia	7.3	FALSE	1
Mesocricetus auratus	Golden hamster	Rodentia	3.9	FALSE	1
Mus musculus	Mouse	Rodentia	4	FALSE	GRCm38
Rattus norvegicus	Rat	Rodentia	3.8	FALSE	6
Ochotona princeps	Pika	Lagomorpha	7	FALSE	3
Oryctolagus cuniculus	Rabbit	Lagomorpha	9	FALSE	2
Gorilla gorilla	Gorilla	Primates	60.1	FALSE	3.1

Species	Common Name	Order	Max. Lifespan (yrs)	Genome mined via MAKER pipeline	Genome Version
Homo sapiens	Human	Primates	122.5	FALSE	GRCh38
Macaca fascicularis	Macaque	Primates	39	FALSE	5
Mandrillus leucophaeus	Drill	Primates	39	FALSE	1
Pan troglodytes	Chimpanzee	Primates	59.4	FALSE	2.1.4
Galeopterus variegatus	Flying squirrel	Dermoptera	NA	FALSE	3.0.2

table S6. Positive selection test results for the RefSeq + MAKER and RefSeq-only data sets. Significant results before and after FDR corrections are shown.

Bat Branch				***Myotis* Branch**				***Rhinolophus ferrumequinum* Branch**				***Miniopterus natalensis* Branch**				**Naked mole rat Branch**			
RefSeq + MAKER		**RefSeq**		**RefSeq + MAKER**		**RefSeq**		**RefSeq + MAKER**		**RefSeq**		**RefSeq + MAKER**		**RefSeq**		**RefSeq + MAKER**		**RefSeq**	
Pre-FDR	**FDR**	**Pre-FDR**	**FDR**	**Pre-FDR**	**FDR**	**Pre-FDR**	**FDR**	**Pre-FDR**	**FDR**	**Pre-FDR**	**FDR**	**Pre-FDR**	**FDR**	**Pre-FDR**	**FDR**	**Pre-FDR**	**FDR**	**Pre-FDR**	**FDR**
NCL	none	*NCL*	none	*HORMAD1*	none	*GNL3L*	*SIRT2*	none	none	NA	NA	*MAP3K4*	none	*MAP3K4*	none	*FANCA*	none	*CCDC79*	none
TEP1		*TP53BP1*		*MYC*		*MSH2*	*TNKS1BP1*					*NUP98*		*POT1*		*LIG1*		*FANCA*	
TP53BP1		*TPP1*		*POLA2*		*SIRT2*						*POLD1*		*PRKDC*		*PINX1*		*LIG1*	
TPP1				*PRKDC*		*TNKS1BP1*						*POT1*		*SLX4*		*PMS2*		*PINX1*	
				RBL2								*PRKDC*		*SMG1*		*PRKDC*		*PMS2*	
				STAG3								*SLX4*				*SPATA22*		*PRKDC*	
												SMG1				*WRN*		*SPATA22*	
																		WRN	

table S7. Divergent selection test results for the RefSeq + MAKER and RefSeq-only data sets. Significant results before and after FDR corrections are shown. Underlined genes that were significant in both data sets after FDR correction are considered robust.

Bat Branch				***Myotis* Branch**				***Rhinolophus ferrumequinum* Branch**				***Miniopterus natalensis* Branch**				**Naked mole rat Branch**			
RefSeq + MAKER		**RefSeq**		**RefSeq + MAKER**		**RefSeq**		**RefSeq + MAKER**		**RefSeq**		**RefSeq + MAKER**		**RefSeq**		**RefSeq + MAKER**		**RefSeq**	
Pre-FDR	**FDR**	**Pre-FDR**	**FDR**	**Pre-FDR**	**FDR**	**Pre-FDR**	**FDR**	**Pre-FDR**	**FDR**	**Pre-FDR**	**FDR**	**Pre-FDR**	**FDR**	**Pre-FDR**	**FDR**	**Pre-FDR**	**FDR**	**Pre-FDR**	**FDR**
CBX5	*MYC*	*CBX5*	*MYC*	*ATM*	*ATM*	*ATM*	*ATM*	*CCT2*	none	NA	NA	*CBX5*	*CCT5*	*CCT5*	*CCT5*	*BRIP1*	none	*BRIP1*	none
DPY30		*CCDC155*		*ATP5C1*	*ATP5C1*	*ATP5C1*	*SETX*	*DOT1L*				*CCT4*	*HNRNPU*	*DNA2*	*DNA2*	*CCDC155*		*CCDC155*	
ERCC1		*ERCC1*		*ATRX*	*SETX*	*ATRX*		*DPY30*				*CCT5*	*LIG1*	*FANCL*	*FANCL*	*DMC1*		*CDC45*	
FANCC		*FANCC*		*CCDC155*		*CCDC155*		*GNL3L*				*DNA2*		*HNRNPD*	*HNRNPD*	*DPY30*		*DMC1*	
MAEL		*KRAS*		*CCT4*		*CCT4*		*HNRNPA2B1*				*DPY30*		*HNRNPU*	*HNRNPU*	*EGF*		*EGF*	
MAP3K4		*MAEL*		*CCT5*		*CCT5*		*RNF8*				*FANCL*		*LIG1*	*LIG1*	*HNRNPA2B1*		*MLH1*	
MYC		*MYC*		*CHEK2*		*CHEK2*						*HNRNPD*		*NEK7*		*MLH1*		*MRE11A*	
NEK7		*NEK7*		*DNA2*		*DNA2*						*HNRNPU*		*NSMCE1*		*MRE11A*		*MSH4*	
PARP1		*PARP1*		*DPY30*		*HORMAD1*						*LIG1*		*NUP98*		*MSH4*		*NBN*	
PLA2R1		*PLA2R1*		*HNRNPA2B1*		*KRAS*						*NEK7*		*PLA2R1*		*NBN*		*POLD1*	
PNKP		*PNKP*		*HORMAD1*		*MEI4*						*NSMCE1*		*PRKCA*		*NDC1*		*RB1*	
RAD50		*RAD50*		*MEI4*		*NAT10*						*NSMCE4A*		*RPA1*		*NSMCE2*		*SDE2*	
SMC5		*SMC5*		*NAT10*		*NBN*						*NUP98*		*RPA3*		*POLD1*		*TDG*	
SMG5		*SMG5*		*NBN*		*NDC1*						*PLA2R1*		*SMC5*		*RB1*		*TGFB1*	
TGFB1		*TGFB1*		*NDC1*		*NEK7*						*PRKCA*		*TCP1*		*SDE2*		*YLPM1*	
TNKS1BP1		*TNKS1BP1*		*NEK7*		*POLA2*						*RAD51C*				*TDG*			
TP53BP1		*TP53BP1*		*POLA2*		*PRIM2*						*RPA3*				*TGFB1*			
XRCC3		*XRCC3*		*SETX*		*SETX*						*TCP1*				*YLPM1*			
		YLPM1		*TELO2*		*TELO2*													
				TERT		*TERT*													
				TP53		*TP53*													

table S8. Detailed model output and R^2 values for LMMs fitted to data sets with the 0-age cohort removed to facilitate a comparison of slopes (effect sizes).

Species	Models Tested	Ranked AIC	Random Variables	Fixed Effect	Estimate	Std. Error	t-value	*p*-value	R^2 - Marginal	R^2 - Conditional
Myotis myotis	LMM	17.13	DNA Plate, Assay Plate and Year Sampled	Intercept	1.425	0.095	15.067	0.003	0.011	0.422
				Age	-0.020	0.013	-1.499	0.136		
Myotis bechsteinii	LMM	107.93	DNA Plate, Assay Plate	Intercept	2.817	0.649	4.342	0.213	0.004	0.850
				Age	-0.021	0.019	-1.119	0.270		
Rhinolophus ferrumequinum	LMM	-144.54	DNA Plate and Assay Plate and Year Sampled	Intercept	1.025	0.255	4.022	0.147	0.008	0.919
				Age	-0.008	0.002	-3.384	0.001***		
Miniopterus schreibersii	LMM	-96.19	DNA Plate and Assay Plate	Intercept	1.205	0.021	57.063	0.000	0.206	0.332
				Age	-0.005	0.002	-2.501	0.027 *		

table S9. Results of pairwise comparisons of DEGs in *Myotis* compared to other mammals across tissue types.

Brain			
Pairwise comparison	**Up-regulated**	**Down-regulated**	**Non-significant**
Myotis vs Cow	6	76	94
Myotis vs Human	65	4	120
Myotis vs Mouse	75	13	90
Myotis vs Naked mole rat	72	5	114
Myotis vs Rat	58	10	110
Blood			
Pairwise comparison	**Up-regulated**	**Down-regulated**	**Non-significant**
Myotis vs Human	129	5	55
Myotis vs Mouse	110	7	65
Myotis vs Pig	74	17	66
Liver			
Pairwise comparison	**Up-regulated**	**Down-regulated**	**Non-significant**
Myotis vs Cow	8	99	69
Myotis vs Human	69	7	113
Myotis vs Mouse	86	18	78
Myotis vs Naked mole rat	79	12	100
Myotis vs Pig	38	20	99
Myotis vs Rat	61	14	103
Myotis vs Whale	22	47	120
Kidney			
Pairwise comparison	**Up-regulated**	**Down-regulated**	**Non-significant**
Myotis vs Cow	7	97	72
Myotis vs Human	89	4	96
Myotis vs Mouse	88	18	76
Myotis vs Naked mole rat	98	5	88
Myotis vs Pig	43	16	98
Myotis vs Rat	73	12	93
Myotis vs Whale	20	59	110

table S10. GO terms corresponding to biological processes which are significantly enriched in the telomere maintenance protein-protein interaction network.

Pathway ID	Pathway Description	Observed Gene Count	FDR	Matching proteins in the network
GO.0032200	telomere organization	10	1.11E-15	ATM, MRE11A, PARP1, RAD50, RFC3, RPA1, TERF2IP, WRAP53, WRN, XRCC5
GO.0000723	telomere maintenance	9	1.10E-13	ATM, MRE11A, PARP1, RAD50, RFC3, RPA1, TERF2IP, WRN, XRCC5
GO.0006281	DNA repair	12	3.34E-12	ABL1, ATM, DCLRE1A, MLH3, MRE11A, PARP1, RAD50, RFC3, RPA1, SETX, WRN, XRCC5
GO.0051276	chromosome organization	13	2.84E-10	ATM, MLH3, MRE11A, PARP1, RAD50, RB1, RFC3, RPA1, SETX, TERF2IP, WRAP53, WRN, XRCC5
GO.0006974	cellular response to DNA damage stimulus	12	5.16E-10	ABL1, ATM, DCLRE1A, MLH3, MRE11A, RAD50, RFC3, RPA1, SETX, TERF2IP, WRN, XRCC5
GO.0006302	double-strand break repair	8	9.93E-10	ATM, MRE11A, PARP1, RAD50, RPA1, SETX, WRN, XRCC5
GO.0006310	DNA recombination	8	1.52E-08	MLH3, MRE11A, RAD50, RFC3, RPA1, SETX, WRN, XRCC5
GO.0060249	anatomical structure homeostasis	8	1.92E-07	ATM, MRE11A, PARP1, RAD50, RFC3, TERF2IP, WRN, XRCC5
GO.0010833	telomere maintenance via telomere lengthening	5	3.33E-07	MRE11A, RAD50, RFC3, RPA1, TERF2IP
GO.0006259	DNA metabolic process	10	3.37E-07	ABL1, DCLRE1A, MLH3, MRE11A, RAD50, RFC3, RPA1, SETX, TERF2IP, XRCC5
GO.0006284	base-excision repair	5	1.42E-06	MRE11A, PARP1, RFC3, RPA1, WRN
GO.0032508	DNA duplex unwinding	5	1.79E-06	MRE11A, RAD50, SETX, WRN, XRCC5
GO.0006260	DNA replication	6	3.03E-05	MRE11A, RAD50, RFC3, RPA1, TERF2IP, WRN
GO.0007131	reciprocal meiotic recombination	4	3.03E-05	ATM, MLH3, MRE11A, RAD50
GO.0007004	telomere maintenance via telomerase	3	0.000117	MRE11A, RAD50, TERF2IP
GO.0000724	double-strand break repair via homologous recombination	4	0.000588	ATM, MRE11A, RAD50, RPA1
GO.0042592	homeostatic process	9	0.00079	ATM, MRE11A, PARP1, RAD50, RB1, RFC3, TERF2IP, WRN, XRCC5
GO.0006298	mismatch repair	3	0.00137	ABL1, MLH3, RPA1

Pathway ID	Pathway Description	Observed Gene Count	FDR	Matching proteins in the network
GO.0040009	regulation of growth rate	2	0.00166	PARP1, WRN
GO.0042769	DNA damage response, detection of DNA damage	3	0.0029	PARP1, RFC3, RPA1
GO.0000019	regulation of mitotic recombination	2	0.00307	MRE11A, RAD50
GO.0030097	hemopoiesis	6	0.00332	ABL1, ATM, PARP1, RB1, RPA1, XRCC5
GO.0070192	chromosome organization involved in meiosis	3	0.00427	MLH3, MRE11A, RAD50
GO.0000018	regulation of DNA recombination	3	0.0102	MRE11A, RAD50, TERF2IP
GO.0002327	immature B cell differentiation	2	0.0114	ABL1, ATM
GO.0006975	DNA damage induced protein phosphorylation	2	0.0114	ABL1, ATM
GO.1902589	single-organism organelle organization	9	0.0128	DCLRE1A, MRE11A, PARP1, RAD50, RB1, RFC3, TERF2IP, WRN, XRCC5
GO.0000280	nuclear division	5	0.0182	ABL1, ATM, DCLRE1A, RB1, RPA1
GO.0065009	regulation of molecular function	10	0.0203	ABL1, ATM, DOT1L, MRE11A, PARP1, RAD50, RB1, TERF2IP, WRAP53, WRN
GO.0090304	nucleic acid metabolic process	12	0.0203	ABL1, DCLRE1A, MLH3, MRE11A, RAD50, RB1, RFC3, RPA1, SSB, TERF2IP, WRN, XRCC5
GO.0000731	DNA synthesis involved in DNA repair	2	0.0218	RFC3, WRN
GO.0006289	nucleotide-excision repair	3	0.0218	DCLRE1A, RFC3, RPA1
GO.0090305	nucleic acid phosphodiester bond hydrolysis	4	0.0218	DCLRE1A, MRE11A, RAD50, WRN
GO.0007095	mitotic G2 DNA damage checkpoint	2	0.0249	ATM, MRE11A
GO.0044710	single-organism metabolic process	12	0.0249	ABL1, ATM, DCLRE1A, MLH3, MRE11A, RAD50, RFC3, RPA1, SETX, TERF2IP, WRN, XRCC5
GO.0071897	DNA biosynthetic process	3	0.0249	RFC3, RPA1, WRN
GO.0006261	DNA-dependent DNA replication	3	0.0252	RFC3, RPA1, WRN
GO.0000278	mitotic cell cycle	6	0.0271	ABL1, ATM, DCLRE1A, RB1, RFC3, RPA1
GO.0006996	organelle organization	10	0.0274	DCLRE1A, MRE11A, RAD50, RB1, RFC3, SETX, TERF2IP, WRAP53, WRN, XRCC5

Pathway ID	Pathway Description	Observed Gene Count	FDR	Matching proteins in the network
GO.0016925	protein sumoylation	3	0.0282	PARP1, RPA1, WRN
GO.0051338	regulation of transferase activity	6	0.0363	ABL1, ATM, MRE11A, RAD50, RB1, WRAP53
GO.0071480	cellular response to gamma radiation	2	0.0366	ATM, WRN
GO.0006297	nucleotide-excision repair, DNA gap filling	2	0.0374	RFC3, RPA1
GO.0031954	positive regulation of protein autophosphorylation	2	0.0374	MRE11A, RAD50
GO.0051052	regulation of DNA metabolic process	4	0.0374	MRE11A, RAD50, TERF2IP, WRAP53
GO.0070987	error-free translesion synthesis	2	0.0374	RFC3, RPA1
GO.0042276	error-prone translesion synthesis	2	0.0404	RFC3, RPA1
GO.0006303	double-strand break repair via nonhomologous end joining	2	0.0441	MRE11A, XRCC5
GO.0002520	immune system development	5	0.0459	ABL1, PARP1, RB1, RPA1, XRCC5
GO.0032201	telomere maintenance via semi-conservative replication	2	0.0463	RFC3, RPA1
GO.0098813	nuclear chromosome segregation	3	0.0492	MLH3, MRE11A, RB1

table S11. KEGG pathways which are significantly enriched in the telomere maintenance protein-protein interaction network.

Pathway ID	Pathway Description	Gene Count	FDR	Matching proteins in the network
3450	Non-homologous end-joining	3	7.60E-05	MRE11A, RAD50, XRCC5
3430	Mismatch repair	3	0.000234	MLH3, RFC3, RPA1
3440	Homologous recombination	3	0.000257	MRE11A, RAD50, RPA1
4110	Cell cycle	3	0.0178	ABL1, ATM, RB1
3030	DNA replication	2	0.0336	RFC3, RPA1
3420	Nucleotide excision repair	2	0.0484	RFC3, RPA1

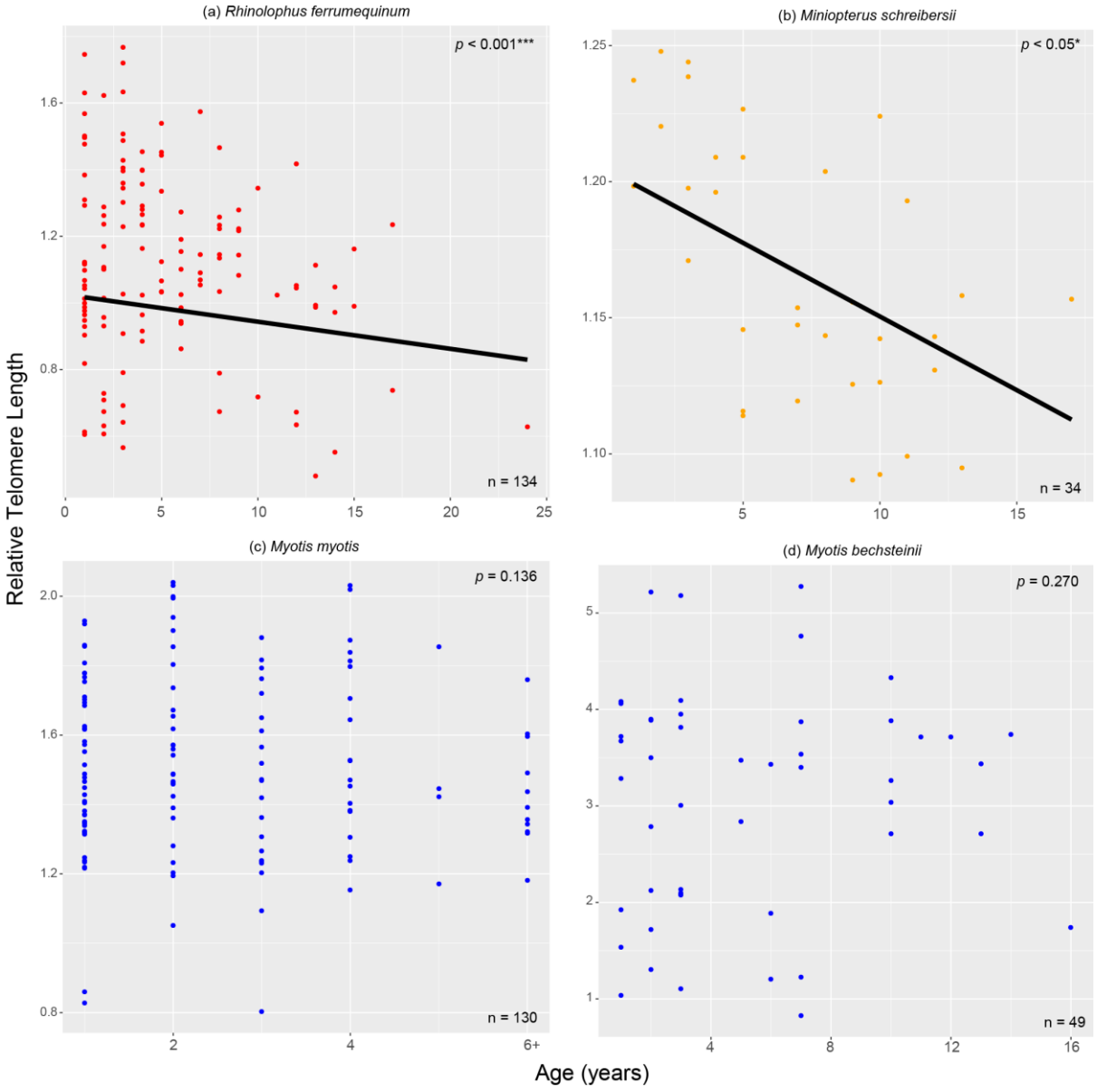

fig. S1. LMMs fitted to each data set after the removal of the 0-age cohort. These results are consistent with the analysis of the data sets with the 0 age cohort included.

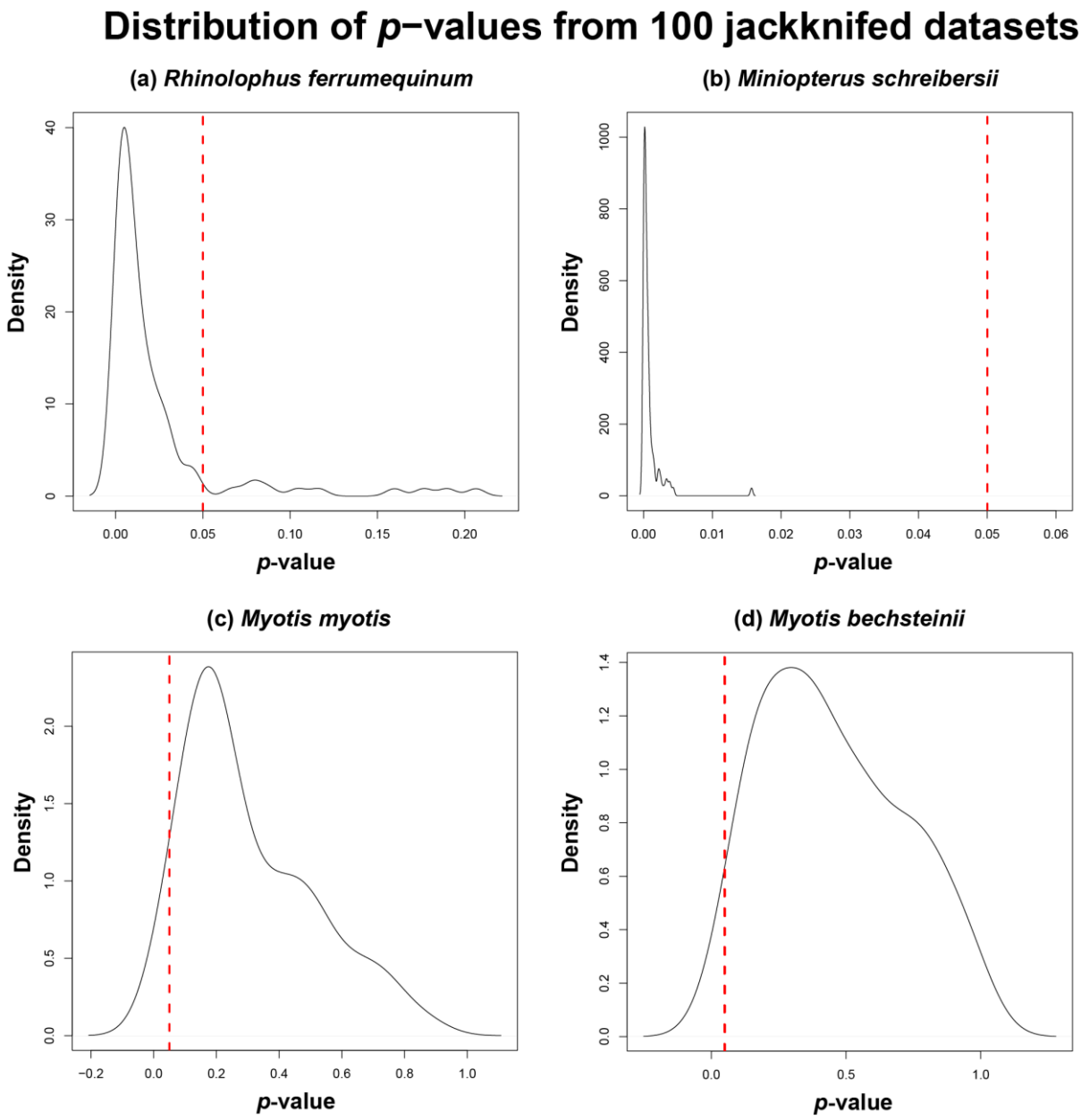

fig. S2. Analysis of *P* values arising from 100 jackknifed models of telomere length versus age. Posterior density distributions of 100 *P* values obtained through jackknife analyses of telomere length vs age models for a) *R. ferrumequinum*, b) *M. schreibersii*, c) *M. myotis* and d) *M. bechsteinii*. Results to the left of the red line at 0.05 are significant. Note that scales differ between plots.

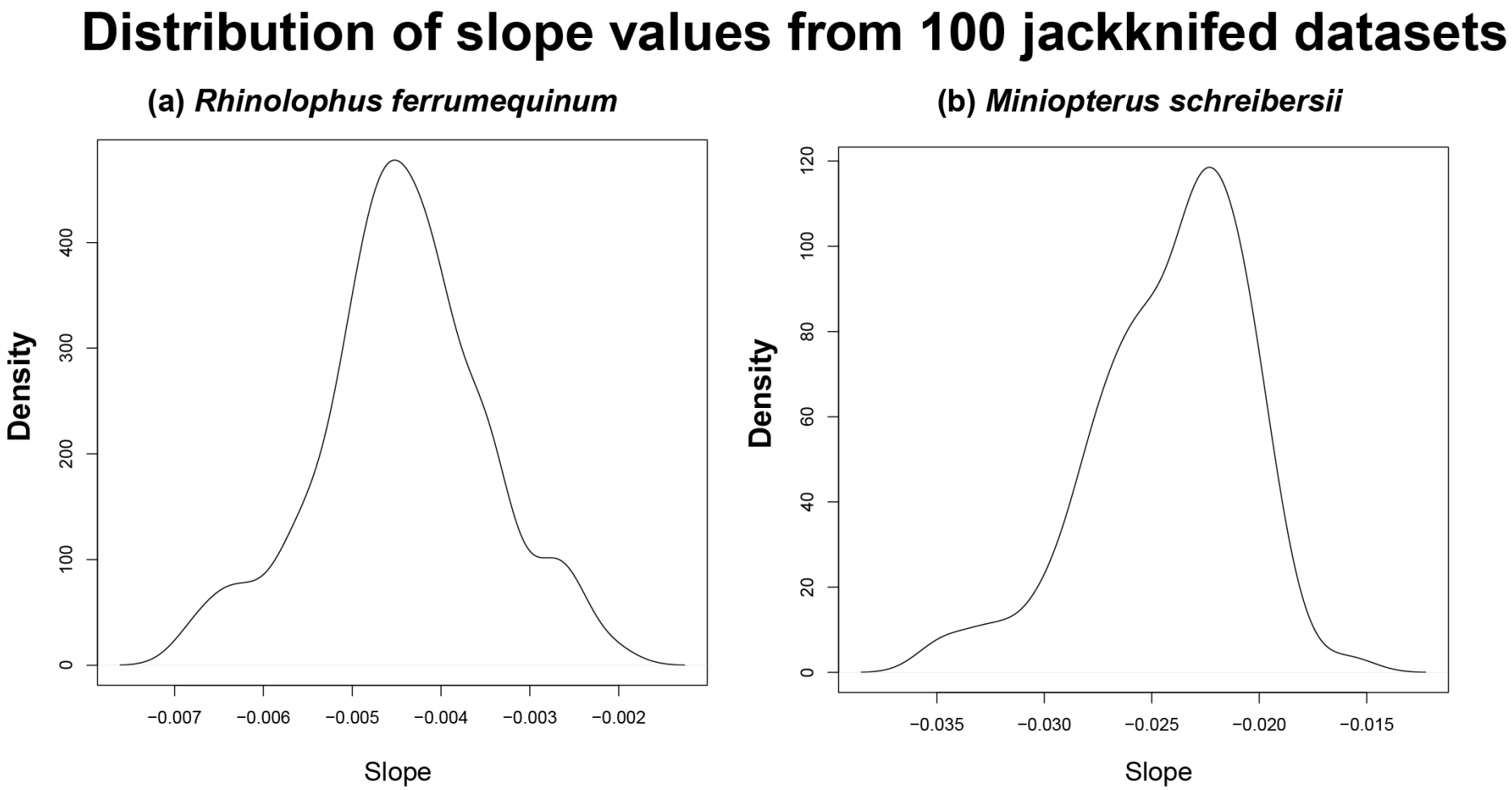

fig. S3. Analysis of slope values arising from 100 jackknifed models of telomere length versus age. Posterior density distributions of 100 effect sizes/slopes (proxy for telomere shortening rate) obtained through jackknife analyses of telomere length vs age models for a) *R. ferrumequinum* and b) *M. schreibersii*.

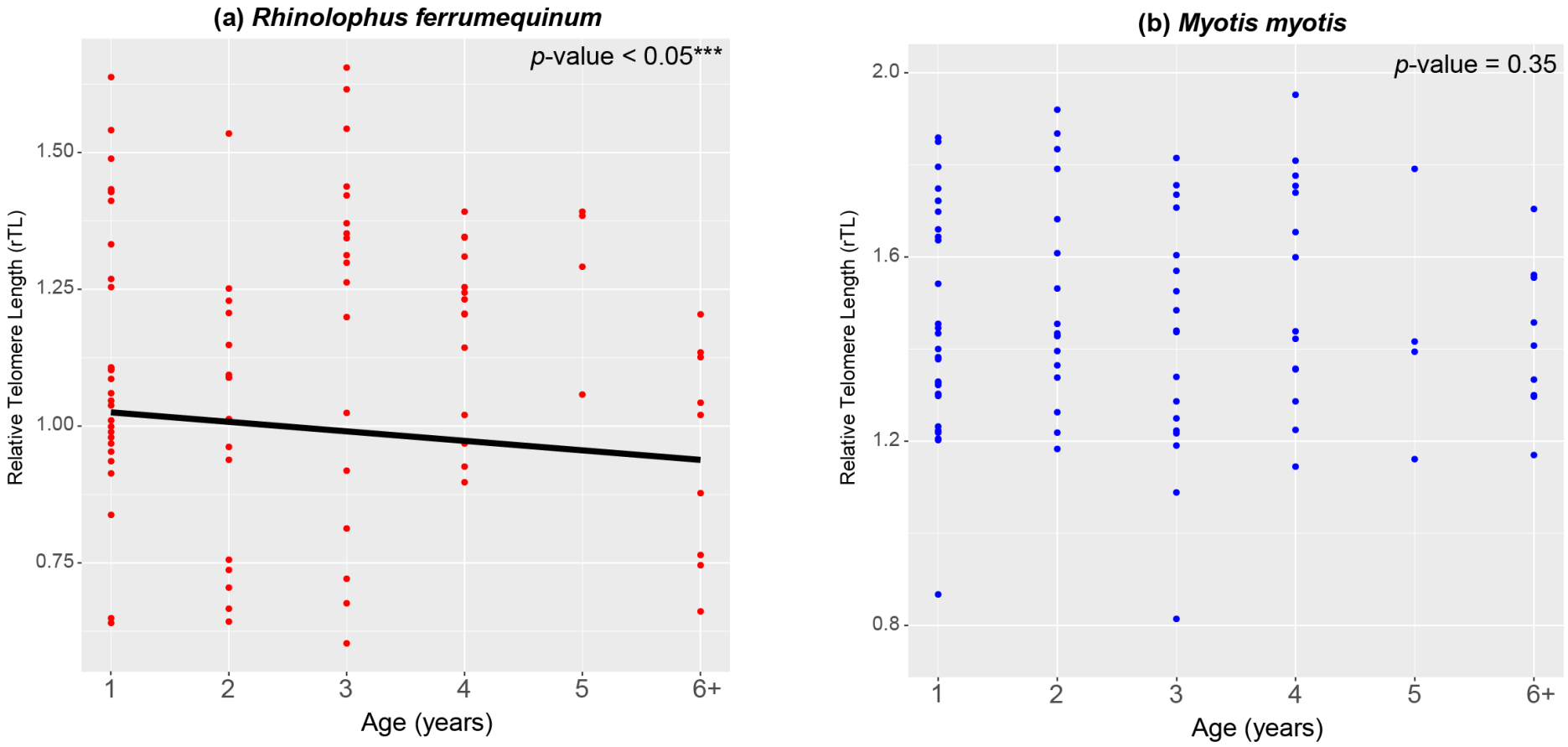

fig. S4. Randomly subsampled *M. myotis* and *R. ferrumequinum* data sets containing equal numbers of samples per age cohorts recapitulate results from Fig. 2 and show telomeres shorten in *R. ferrumequinum*, but we do not detect a significant relationship between rTL and age in *M. myotis*. Note that scales differ between plots.

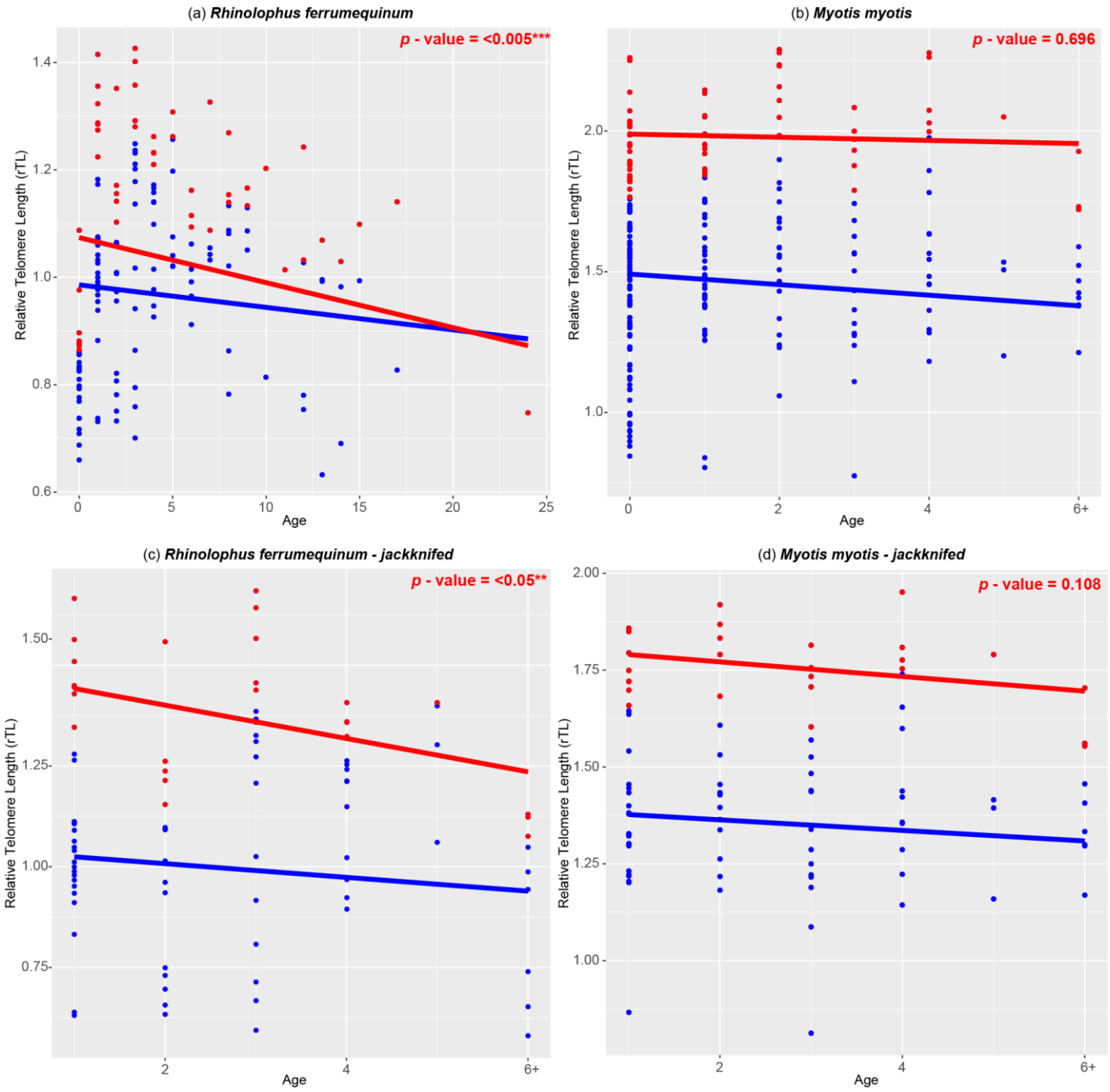

fig. S5. Upper quartile regression analysis. Upper quartile regression for (**a**) *R. ferrumequinum* and (**b**) *M. myotis* data sets shown in Fig. 2 and jackknifed data sets for (**c**) *R. ferrumequinum* and (**d**) *M. myotis* data sets shown in fig. S3. Upper quartile samples are highlighted in red and red lines represent the fitted upper quartile models for all data sets. *P* values are shown for upper regression models. Note that scales differ between plots.

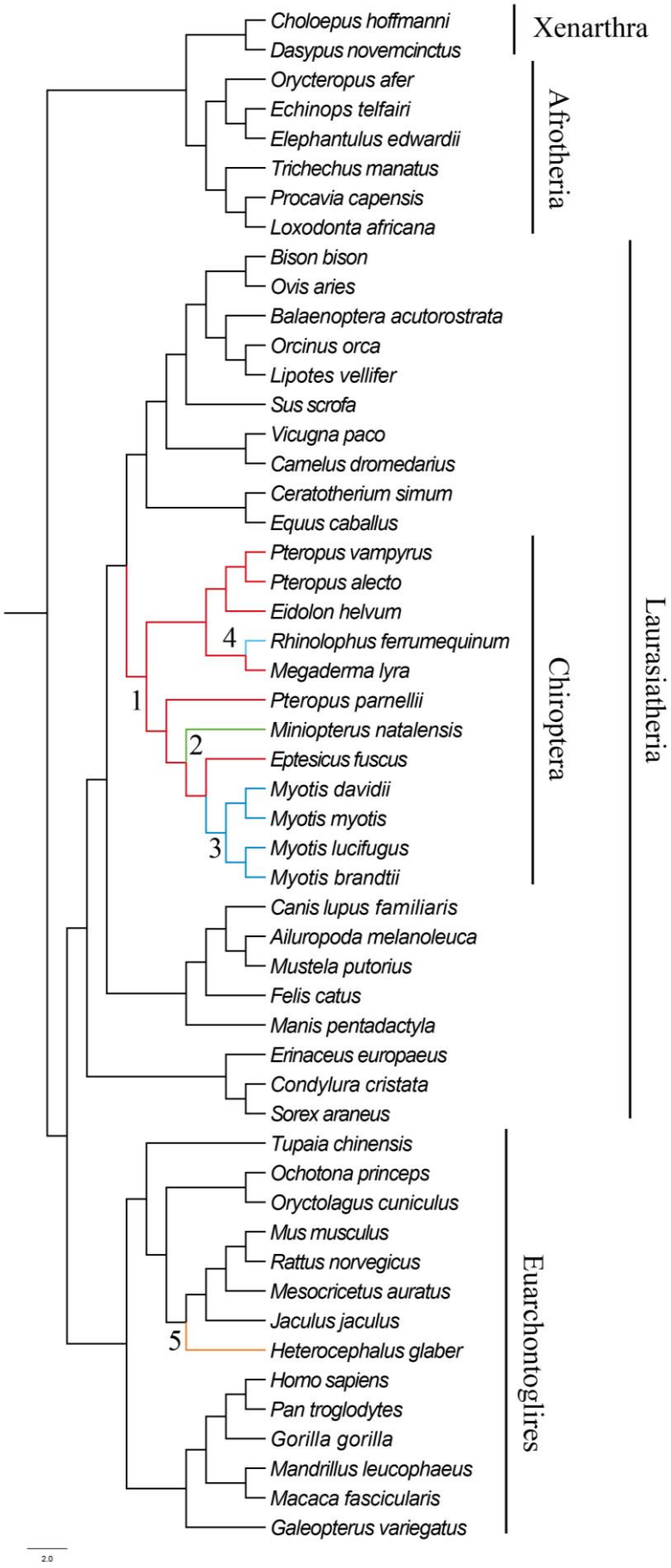

fig. S6. Tree topology used for selective pressure analyses. Branches tested are colour coded and labelled 1-5.

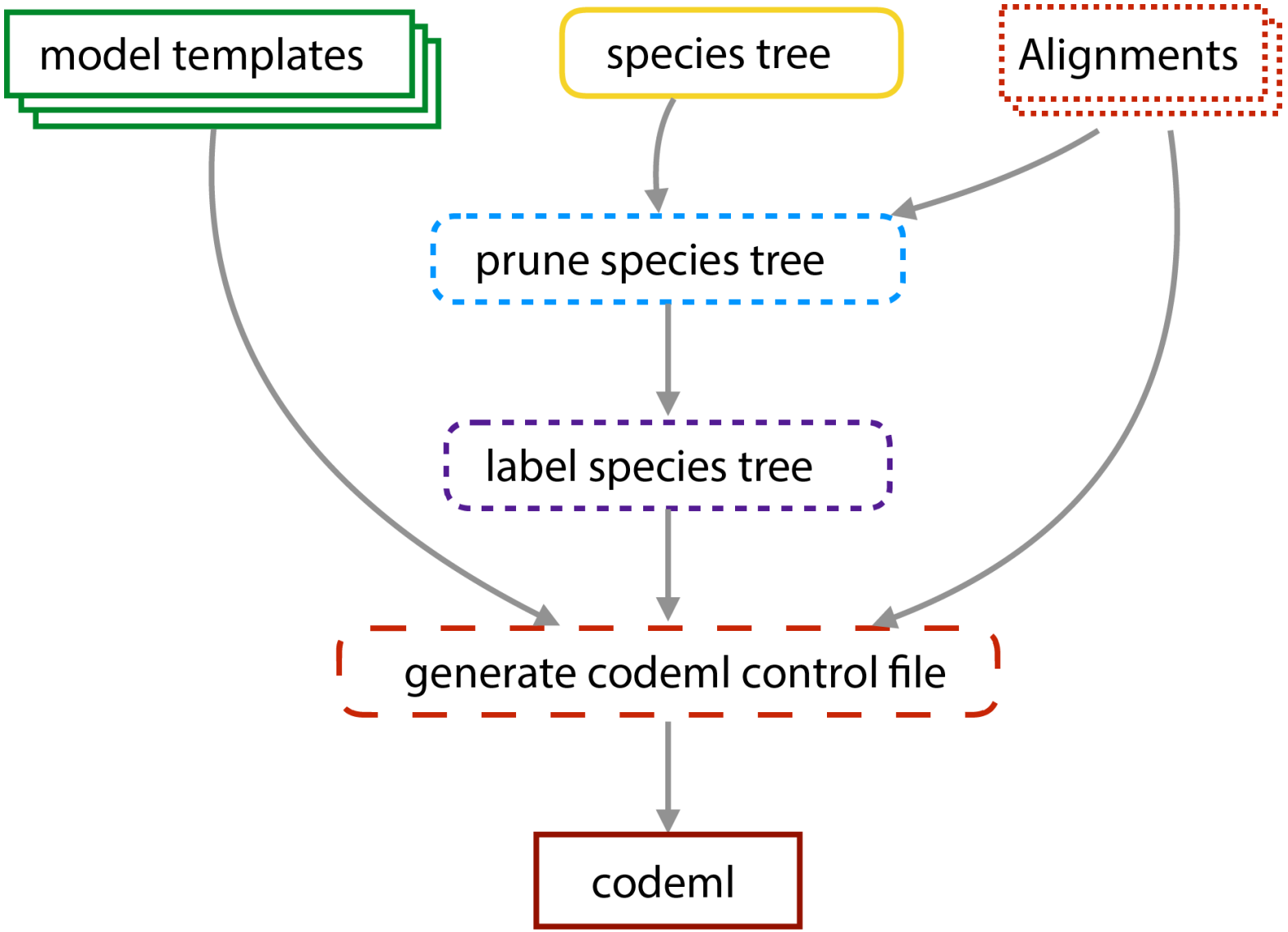

fig. S7. Schematic depicting steps in the OH-SNAP workflow to automate CodeML analysis.

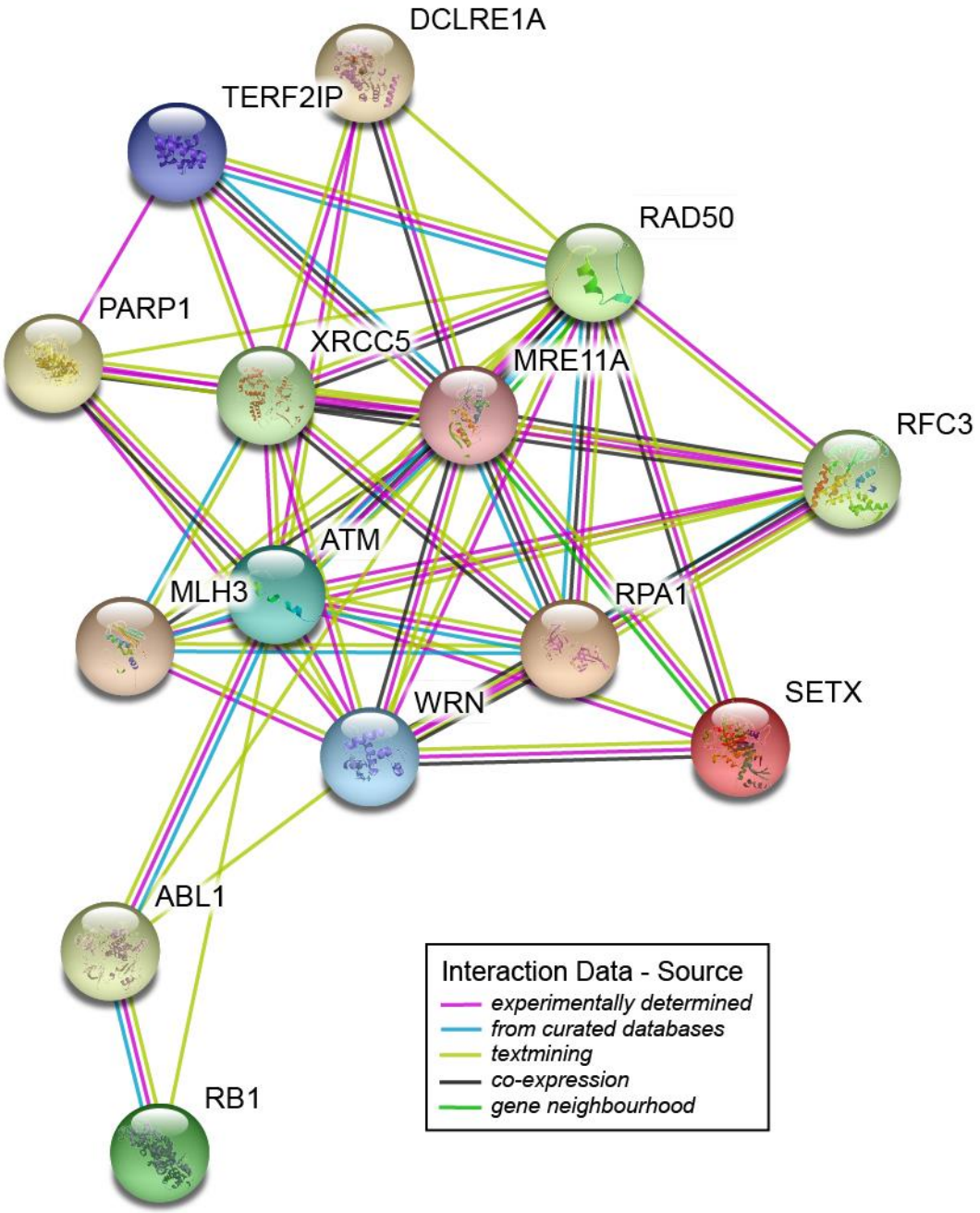

fig. S8. STRING protein-protein-interaction network for 14 significantly DEGs in *Myotis* bats compared to all other mammals. The network depicts direct interaction between 14 telomere maintenance proteins with additional functions in DNA repair.